Determination of Fiber Content in 3D Printed Composite Parts Using Image Analysis

Harsh Srivastava, Hammond Pearce (Member, IEEE), Gary Mac, and Nikhil Gupta, (Senior Member, IEEE).

Abstract—Fiber-reinforced composite parts used in drones, automobiles, and sports equipment are now being manufactured by additive manufacturing (AM), where the material parameters such as fiber direction can be changed within a layer or from one layer to the other. Non-destructive evaluation methods are required to assess the quality of such customized printed parts. In this work, a micro-computed tomography (µCT) dataset is analyzed to determine the fiber content in a 3D printed composite material part using a digital binary image processing method. The existing literature on binary image analysis methods to measure the fiber volume fraction is limited to continuous fiber reinforced composites. Discontinuous fiber reinforced 3D printing filaments are popular in manufacturing parts with increased strength. The methods developed in this work expands the binary image process to scans that show fibers embedded length-wise in different directions in the 3D printed layers. An optimized thresholding method is trained on the filament sample and then applied to 3D printed samples. The results show fiber volume fraction measurements with standard deviations below 0.15%. The results in this work will be useful for product quality validation.

Index Terms—Additive manufacturing, cyber-physical system, non-destructive evaluation, composite material.

I. INTRODUCTION

Additive manufacturing (AM) technologies continue to make advancements in improving the quality of the printed product, development of novel materials for printing and increasing the printing speed. Many extrusion-based 3D printers can be used to print composite material parts by using glass and carbon fiber-reinforced composite material filaments [1]. Composite material filaments are widely available for use in the fused filament fabrication (FFF) 3D printers and there are many advantages over traditional filaments [2].

Parts printed with fiber-reinforced polymer (FRP) composite material can be strong, lightweight, and functional. The mechanical strength of these FRP composite parts depends on the volume fraction and orientation of reinforcing fibers in the structure of the part [3]. These parameters depend on controlling the AM process settings such as the toolpath and layer thickness, which will lead to different material response

Manuscript received October 1, 2021. This work was supported in part by the U.S. National Science Foundation grant OISE-1952479 and SecureAmerica Institute grant.

- H. Srivastava was with Dept. of Chemical Engineering, National Institute of Technology Warangal, Telangana 506004 India.
- H. Pearce was with the Dept. of Electrical and Computer Engineering, New York University, Brooklyn NY 11201 USA.
- G. Mac (corresponding author, e-mail: gm1247@nyu.edu) was with the Dept. of Mechanical and Aerospace Engineering, New York University, Brooklyn NY 11201 USA.
- N. Gupta was with the Dept. of Mechanical and Aerospace Engineering, New York University, Brooklyn NY 11201 USA.

under the designated loading conditions [4], [5]. The raster angle of each layer of the printed part controls the fibers' orientation and the density of the infill governs the part's overall fiber volume fraction (ϕ_i) . The process of quality assessment of these parts, which often cannot be mechanically tested, need to be non-destructively tested for verification of material and properties. Past work involved reverse engineering an AM produced part through machine learning and non-destructive imaging to determine the fibers' orientation [6].

The fiber orientation can vary across each layer in a 3D printed composite part and imaging of these short, discontinuous fibers often result in a large amount of data. Machine learning algorithm is a great tool to help analyze a large image dataset with the advantages of automation, easy identification of patterns, and continuous improvements in accuracy. The successful development of a machine learning algorithm is highly dependent on robust training of the parameters and being able to confirm the accuracy of the results. In digital image analysis of fibers in printed parts, the important parameter to optimize is the threshold range to correctly separate the fiber, resin, and voids in the image.

In this work, a FFF 3D printer is used for AM of FRP composite specimens, which were subjected to imaging using a micro-computed tomography (μ CT) scanner. The specimens contained short glass fibers mixed with the filament. The image dataset obtained from μ CT is used to determine the ϕ_f in the specimens using image analysis methods. The successful classification of fiber content using non-destructive techniques can be expanded to include defect detections in AM produced parts for reliable manufacturing.

II. BACKGROUND

Determining the ϕ_f in composite materials has long been of interest to manufacturers and researchers. Both destructive and non-destructive methods have been used for this purpose. Among the destructive methods, burn-off and acid digestion tests are commonly used to remove the polymer and the remaining fibers are weighed to determine the ϕ_f . The fiber content measured from these methods is useful in obtaining the void content in the manufactured part [7], [8]. In addition, the ϕ_f can be used in theoretical modeling with finite element analysis for realistic predictions [9]. Since these methods are destructive in nature, they cannot be used on the end-use production parts. Certain polymers release hazardous gases when exposed to high temperatures for a prolong period and may not be suitable for burn-off tests.

Non-destructive evaluation (NDE) methods such as ultrasonic imaging and μ CT scanning are widely used for imaging the specimens and determining the microstructure and defects. [10], [11]. X-ray μ CT have been used for

microstructural analysis of short fiber reinforced thermoplastics using an algorithm relying on iterative single fiber segmentation [12]. Optical microscopy-based image analysis technique has been proven to be able to characterize ϕ_f and show great results when compared with the traditional acid digestion method [13], [14]. The ϕ_f of FRP composites has also been successfully characterized with the use of scanning electron microscope and digital image processing [15], [16].

Microscopy is a destructive imaging method, where the surface features may be dependent on the method used for specimen cutting and preparation. Fiber counting methods performs the analysis on the cross section of the fibers in the images and single fibers may be mistakenly segmented into multiple fibers. Specimens need to be prepared and imaged in a specific orientation to be able to view the cross sections of fibers. The burn-off method is not suitable for the filament used in this work due to the release of hazardous gases, carbon monoxide and hydrogen cyanide. An NDE imaging approach is proposed to determine the ϕ_f in printed tensile test specimens of two different raster angle. As the selection of the optimal threshold value for segmenting the fibers in binary image methods is very subjective, the threshold parameter needs to be trained for accurate determination of ϕ_f in printed parts.

III. METHODOLOGY

A. AM Fiber-reinforced Composite Test Samples

The computer-aided design (CAD) model of the tensile test specimen is designed using SolidWorks 2020 and follows the subsize specimen dimensions of the ASTM E8/E8M standard. The overall length, thickness, and width of grip section of the tensile test specimen samples were 4, 0.25, and 0.375 in, respectively. The stereolithography file format of the sample is imported into the Ultimaker Cura slicing application. In Cura, two different raster angles are set for the printed samples. Fig. 1 shows the printing direction parameter and Sample A is printed with angles of 90° and 0° for each odd and even layer, respectively. Sample B is printed with all layers being unidirectional in the 0° orientation. The printing parameter of both samples include 100% infill density, printing temperature of 240°C, build plate temperature of 90°C, and a layer height of 0.25 mm. Cura outputs a g-code file, which contains all the processing parameters and the set of instructions for the 3D printer.

The samples are printed on a FlashForge FFF 3D printer using a glass fiber-reinforced acrylonitrile butadiene styrene (ABS) filament of 1.75 mm diameter manufactured by 3DXTECH (Grand Rapids, Michigan, USA). The ABS filament contains 10 vol.% of glass fiber. A small piece was cut from the ends of the printed sample using a diamond saw blade for the μCT scan. Each samples is mounted in a SkyScan 1172 μCT scanner to obtain the images showing the fibers at each layer. The scan was conducted using camera pixel size of 9 μm, source voltage of 49 kV, source current of 198 µA, rotation step of 0.4° per scan, and 180° rotation. SkyScan's NRecon reconstruction software is used to produce cross-section slices of the scanned sample using a smoothing value of 2, ring artifact correction value of 10, and beam hardening correction value of 25%. Sample A and B had a total of 258 and 232 images, respectively. The µCT of Sample A was reconstructed without

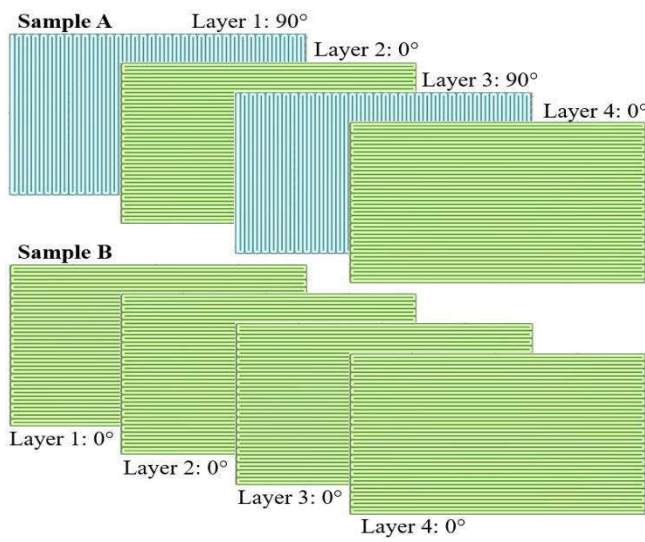


Fig. 1. shows the print direction of the specimens with Sample A depicting layers of alternating angles of 90° (blue) and 0° (green). A unidirectional Sample B with all layers printed in 0° .

a region of interest and Sample B had a circular region of interest applied to all the images.

B. Manual Threshold of Samples

The reconstructed μ CT scans are imported as 8-bit images into ImageJ, an open source Java image processing software. As the μ CT images are grayscale by default, there is no need to convert these images for the binarization process. Ten μ CT images are randomly selected from each dataset of Sample A and B to manually determine the optimal threshold range to capture the pixels that only represents fibers in the printed specimen. Each of the 20 images are manually adjusted to find the threshold range of best fit for fiber pixels with the *dark background* option enabled. The upper bound threshold value was kept at the default value of 255. The lower bound average threshold value is 159 and 182 for Sample A and B image dataset, respectively.

The same procedure is repeated for each of the 20 images to manually find the optimal lower bound threshold value to represent both the resin and fiber pixels. The threshold value is carefully selected to exclude the voids and noises in the μCT images. The lower bound average threshold value to represent fiber and resin together is 82 and 12 for Sample A and B image dataset, respectively.

ImageJ calculates the area of pixels in the μ CT scan after thresholding using the *Analyze Particles* command. A macro is created in ImageJ to automate the process of applying the threshold and calculating the areas for all images in the μ CT image dataset. The ϕ_f is determined by dividing the area of fiber by the total area of both resin and fiber in each image.

C. Automatic Threshold of Samples

There are algorithms in ImageJ to automatically determine the threshold ranges in the image. The MaxEntropy algorithm is used to automatically threshold the μ CT images to find all the pixels that represents fibers by maximizing the inter-class entropy. The maximum entropy threshold is effective to segment images with bright objects on a dark background. The Minimum algorithm is used to select the total area of resin and fiber pixels in the scanned images. The intensity histogram is

iteratively smoothed using a running average of size 3 until there are only two local maxima and the minimum between the two peaks is the threshold value. A macro containing these automatic thresholding algorithms is implement on all 490 images to get the area values from both algorithms.

D. Optimized Threshold Technique

The *Enhance Contrast* function is used to increase the white pixel intensity using a saturated pixel value of 15% and the *normalize* option enabled. Normalization improves the contrast in the image by recalculating the range of intensity values to span the maximum range of 0-255 for 8-bit images. The threshold range is set between 250 and 255 to capture the fiber pixels. The automatic threshold *Minimum* algorithm is used to select the resin and fiber pixels. The optimized threshold technique is performed on the μ CT images to record the calculated areas.

IV. RESULTS

In the reconstructed μ CT images, glass fibers are represented with white pixels, ABS resin matrix is shown as the gray pixels, and voids from the printing process are shown as black pixels. Fig. 2 shows that there is a peak in frequency near the pixel intensity value of 0, 130, and 255 which corresponds with voids, resin, and fibers, respectively. Image binarization is the process of separation of pixels into two distinct groups based on the pixel grayscale intensity value.

Two methods for manual and automatic binarization are used on the image dataset to train the thresholding parameter for the characterization of ϕ_f in 3D printed parts. The manual threshold method of choosing the value to represent a group of pixels is very subjective and the determination of ϕ_f is influenced by user bias. This can be seen by the overestimation of ϕ_f by the manual threshold method in both Sample A and B compared to the reported 10% ϕ_f by the manufacturer. This overestimation is a result of selecting a low threshold range to represent fibers by the user. The automatic threshold methods also overestimate the ϕ_f because these techniques are not optimized for the characterization of ϕ_f . The automatic threshold *Minimum* function did capture most of the pixels representing the fiber and resin in the image while leaving out the voids.

An optimized threshold method is derived from the results of the manual and automatic techniques. It was determined that the reconstructed μ CT leaves intermediate shades of gray in the background and during the threshold method to determine fibers, it results in noise at the perimeter of the specimen. This issue is presented in the μ CT reconstruction of Sample A and it is corrected in Sample B by taking a circular crop of the specimen. The contrast of the μ CT image is increased and a narrower threshold range is used to better capture the fibers. The higher and smaller pixel intensity range ensures that only the white pixels are selected. The manual threshold selection method was including too many gray pixels that did not represent fibers. The *Minimum* algorithm is used for the optimized method to capture the area of both fibers and resin.

Fig. 3 shows all three threshold techniques for a single μ CT image taken from the Sample A dataset. The manual and automatic thresholding to determine fibers and resin are very similar with both showing extraneous pixels exterior to the

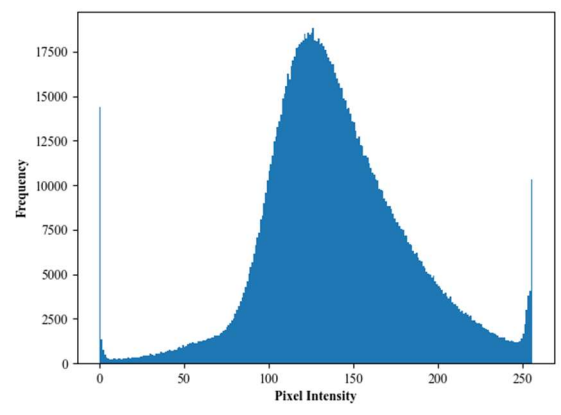


Fig. 2. Histogram of a μ CT image from Sample A showing the distribution of pixels with varying pixel grayscale intensity value.

specimen. The image contrasting caused the optimized threshold method to overestimate the fibers at the corners which can be eliminated with a region of interest. Fig. 4 shows the threshold results for Sample B. The fibers presented in the optimized approach shows improvements over the manual threshold methods. The average ϕ_f from Sample A and B dataset is shown in Table I. The ϕ_f of Sample A and B by the manual method shows a big difference mainly due to the user bias in selecting the threshold value. The algorithm in the automatic method is not providing accurate ϕ_f for Sample B and shows a higher standard deviation in Sample B than in Sample A.

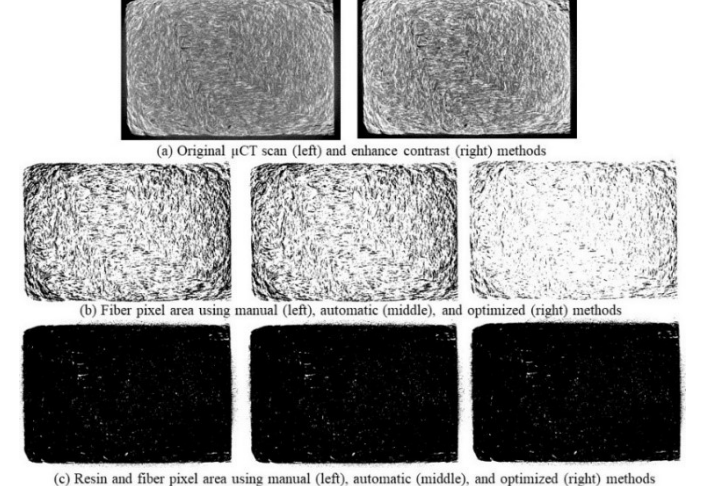


Fig. 3. A comparison of manual, automatic, and optimized threshold techniques on a μCT image of Sample A. (a) μCT of specimen showing fiber, resin, and voids. (b) Thresholding of only fibers. (c) Thresholding of both fiber and resin.

TABLE I
FIBER VOLUME FRACTION COMPARISON OF SAMPLE A AND B

	Sample A		Sample B	
Threshold	Average	Standard Deviation	Average	Standard Deviation
Manual	32.91	1.06	25.25	3.49
Automatic	32.61	1.23	36.55	3.63
Optimized	22.42	0.52	10.63	0.13

The optimized threshold method is tested on several other μ CT dataset shown in Fig. 5. The same images from Sample A dataset were cropped with the reconstruction software and tested using the optimized threshold method. A tensile test specimen was printed with unidirectional layers of 30° angle

and another sample was printed with alternating angles of $45^{\circ}/135^{\circ}$ angles between each layer. A single piece of the glass fiber-reinforced ABS filament was scanned and shows the fiber cross-section in the μ CT image. The calculated ϕ_f based on the

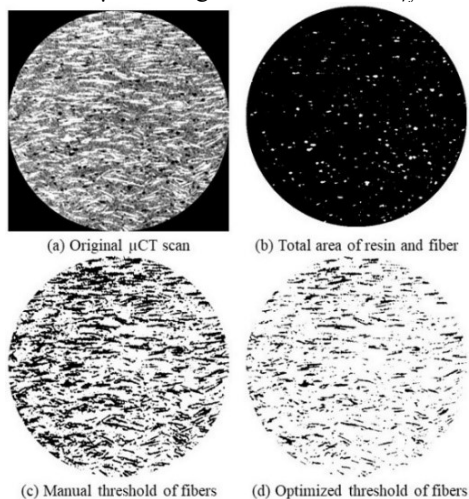


Fig. 4. A result of the threshold methods in determining the area of fibers and resins for a μ CT image of Sample B.

optimized threshold method is shown in Table II. The ϕ_f calculated from different μ CT dataset agree with one another. The higher ϕ_f in the filament dataset shows that the process can further be optimized. Overall, the results proved to be reliable in optimizing the threshold range in binary image analysis and can be the basis for the development of a machine learning algorithm.

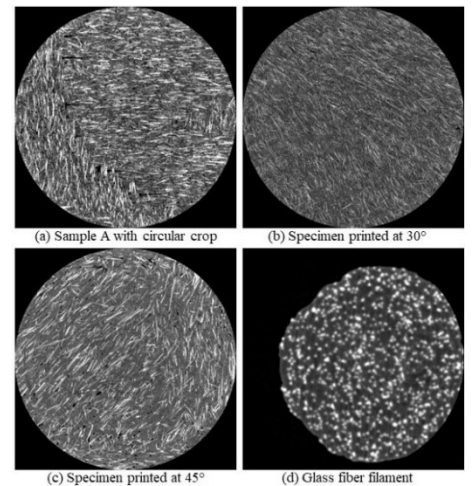


Fig. 5. shows the four μ CT image dataset of printed specimen and filament to test the optimized threshold method.

TABLE II

FIBER VOLUME FRACTION COMPARISON OF TEST DATASET

Seconds A POL 200 450 Estimates

	Sample A ROI	30°	45°	Filament
Average	10.60	10.83	10.61	12.91
Std Dev	0.09	0.15	0.12	0.14

V. CONCLUSIONS

Advancements in 3D printing has made it challenging to assess the quality of the printed parts and determine their properties. This paper demonstrates that using thresholding techniques, the ϕ_f of the composites could be determined, which is vital in estimating the mechanical properties of the

composite. Future work will involve using these results as training data on which machine learning algorithms could be developed to generate predictive models to obtain ϕ_f of any novel raw μ CT images without the need to manually process the μ CT scans in an image processing tools every time.

ACKNOWLEDGMENT

The authors thank the NYU Tandon School of Engineering Makerspace for providing μ CT facilities and Kaushik Yanamandra for helping with the μ CT of specimens.

REFERENCES

- [1] X. Wang, M. Jiang, Z. Zhou, J. Gou, and D. Hui, "3D printing of polymer matrix composites: A review and prospective," *Composites Part B: Engineering*, vol. 110, pp. 442-458, 2017.
- [2] A. K. Singh, B. Patil, N. Hoffmann, B. Saltonstall, M. Doddamani, and N. Gupta, "Additive Manufacturing of Syntactic Foams: Part 1: Development, Properties, and Recycling Potential of Filaments," *JOM*, vol. 70, pp. 303-309, 2018.
- [3] B. Brenken, E. Barocio, A. Favaloro, V. Kunc, and R. B. Pipes, "Fused filament fabrication of fiber-reinforced polymers: A review," *Additive Manufacturing*, vol. 21, pp. 1-16, 2018.
- [4] J. Kiendl, and C. Gao, "Controlling toughness and strength of FDM 3D-printed PLA components through the raster layup," *Composites Part B: Engineering*, vol. 180, p. 107562, 2020.
- [5] G.D.Goh, W. Toh, Y.L.Yap, T.Y.Ng, and W.Y.Yeong, "Additively manufactured continuous carbon fiber-reinforced thermoplastic for topology optimized unmanned aerial vehicle structures," *Composites Part B: Engineering*, vol. 216, p. 108840, 2021.
- [6] K. Yanamandra, G. L. Chen, X. Xu, G. Mac, and N. Gupta, "Reverse engineering of additive manufactured composite part by toolpath reconstruction using imaging and machine learning," *Composites Science* and Technology, vol. 198, p. 108318, 2020.
- [7] M. H. Hassan, A. R. Othman, and S. Kamaruddin, "Void content determination of fiber reinforced polymers by acid digestion method," *Advanced Materials Research*, vol. 795, pp. 64-68, 2013.
- [8] M. H. Hassan, A. R. Othman, and S. Kamaruddin, "The use of response surface methodology (RSM) to optimize the acid digestion parameters in fiber volume fraction test of aircraft composite structures," *The International Journal of Advanced Manufacturing Technology*, vol. 90, pp. 3739 – 3748, 2017.
- [9] U. S. Gupta, M. Dhamarikar, A. Dharkar, S. Tiwari, and R. Namdeo, "Study on the effects of fibre volume percentage on banana-reinforced epoxy composite by finite element method," *Advanced Composites and Hybrid Materials*, vol. 3, pp. 530-540, 2020.
- [10] M. A. Caminero, I. García-Moreno, G. P. Rodríguez, and J. M. Chacón, "Internal damage evaluation of composite structures using phased array ultrasonic technique: Impact damage assessment in CFRP and 3D printed reinforced composites," *Composites Part B: Engineering*, vol. 165, pp. 131 – 142, 2019.
- [11] Q. He, H. Wang, K. Fu, and L. Ye, "3D printed continuous CF/PA6 composites: Effect of microscopic voids on mechanical performance," *Composites Science and Technology*, vol. 191, p. 108077, 2020.
- [12] P. A. Hessman, T. Riedel, F. Welschinger, K. Homberger, and T. Böhlke, "Microstructural analysis of short glass fiber reinforced thermoplastics based on x-ray micro-computed tomography," *Composites Science and Technology*, vol. 183, p. 107752, 2019.
- [13] M.C. Waterbury, and L.T. Drzal, "Determination of fiber volume fractions by optical numeric volume fraction analysis," *Journal of Reinforced Plastics and Composites*, vol. 8, pp. 627–636, 1989.
- [14] M. T. Cann, D. O. Adams, and C. L. Schneider, "Characterization of fiber volume fraction gradients in composite laminates" *Journal of Composite Materials*, vol. 42, pp. 447–466. 2008.
- [15] C. N. Morales, G. Claure, J. Álvarez, and A. Nanni, "Evaluation of fiber content in GFRP bars using digital image processing," *Composites Part B: Engineering*, vol. 200, p. 108307, 2020.
- [16] X.-W. Yu, H. Wang, and Z.-W Wang, "Analysis of yarn fiber volume fraction in textile composites using scanning electron microscopy and xray micro-computed tomography." Journal of Reinforced Plastics and Composites, vol. 38, pp. 199–210, 2019.